Nonlinear Threshold Decrease with Distance in 112 Gb/s PDM-QPSK Coherent Systems

A. Bononi, N. Rossi, P. Serena

Università degli Studi di Parma, Dipartimento di Ingegneria dell'Informazione, v.le G. Usberti 181/A, 43124 Parma (Italy), ✉ bononi@tlc.unipr.it

Abstract *We show that the accumulation rate of nonlinearity in NDM links can also be measured from the nonlinear threshold decrease rate, and provide simulations of such rates for each single- and cross-channel effect.*

Introduction

A nonlinear Gaussian noise model was recently introduced to justify the performance of non-dispersion managed (NDM) coherent links[1,2]. According to that model, performance just depends on the nonlinear signal to noise ratio (SNR) $S = P/(N_A + N_{NLI})$, where P is the power per channel, N_A is the amplified spontaneous emission (ASE) power, and $N_{NLI} = \mathrm{Var}[f_{NLI}] = a_{NL}P^3$ is the variance of the nonlinear interference (NLI) field f_{NLI}, which scales cubically with P through a constant a_{NL}. In a system with N spans, the ASE term scales linearly with N, while the NLI field $f_{NLI} = \sum_{k=1}^{N} f_k$ is the sum of N random variables (RV) contributed by each span. The accumulation law of N_{NLI} with distance N was shown by a frequency-domain analytical model for a Nyquist-spaced wavelength division multiplexed (WDM) system (channel spacing Δf equal to the symbol rate R) to be approximately $N_{NLI} \propto N(1 + \alpha \log N)$ with α a system parameter[3], while a single-channel time-domain analytical model yielded a scaling law $N_{NLI} \propto N \log(kN)$ with k a system parameter[4]. Since the variance N_{NLI} of the NLI field scales as N^1 if the span contributions f_k are uncorrelated RVs, or as N^2 if the span contributions are identical RVs, a pragmatic approximation to the distance scaling law assumes $N_{NLI} \propto N^x$, with x a system factor, whose value reasonably is between 1 and 2. Such a factor was measured from experimental data[5] as $x \cong 1.33$ in 50 GHz spaced, 28 Gbaud polarization division multiplexed quaternary phase shift keying (PDM-QPSK) channels over standard single mode fiber (SMF) NDM links with 100 km spans, and the fit was over the range $5 < N < 30$. For the same system, a value $x \cong 1.25$ over the range $5 < N < 50$ can be read off the simulation results in[6]. The apparent decrease of x when the range of N is extended is confirmed by analysis and simulations in[4]. Such WDM NDM systems have a bandwidth efficiency $\eta = \frac{R}{\Delta f} = 0.56$ and the dominant nonlinear effect is single channel self-phase modulation[7]. Recent experiments[8] performed on ultra-long NDM SMF links with ∼50km spans at variable η confirm that when $\eta \lesssim 0.6$ the NLI accumulation "slope" is $x \cong 1.2 - 1.6$, (since single-channel nonlinear effects are dominant[9]) while at higher η (where presumably cross-nonlinearity dominates) the slope decreases to $x \cong 1.05$. A recent simulation study[10] found that the NLI coefficient a_{NL} can be approximated as the sum of single and cross-channel effects as $a_{NL} = \alpha_{SPM} N^{1.34} + \alpha_{XPM} N^{1.1}$ in the range $1 < N < 30$, where α_{XPM} increases for decreasing channel spacing Δf and eventually gives the dominant contribution as the smallest spacing $\Delta f = R$ is approached, thus indirectly confirming the above experimental findings.

In this paper we want to add to the debate by taking a correlated but different point of view. We already showed how the nonlinear threshold (NLT) at 1dB of SNR penalty $\hat{P}_1$ (i.e., the channel power at which a target bit error rate $BER_0 = 10^{-3}$ is obtained with 1 dB extra SNR with respect to linear propagation) scales with symbol rate R at fixed bandwidth efficiency η and at fixed distance[7,9]. Let S_0 be the SNR required to reach our target BER_0 for the used modulation format. As shown in[4] (Appendix 1), the y dB NLT at $S = S_0$ is

$$\hat{P}_y = \frac{1}{c(y)\sqrt{3 S_0 a_{NL}}} \propto N^{-\frac{x}{2}} \qquad (1)$$

where we used the approximate NLI scaling law $a_{NL} \propto N^x$, and $c(y)$ is a constant (which can be found as in eq. (18) of[4]) depending only on the penalty y, with $c(1) = 1.27$. Such a scaling was already found in[11] for NDM systems with $x = 1$. Hence NDM theory predicts approximately that the plot of NLT versus N in a log-log scale decreases with a slope $-x/2$ dB/dB. We here report on simulation results of $\hat{P}_1$ versus distance

(i.e. versus spans N) at a fixed baudrate $R = 28$ Gbaud and Δf=50 GHz ($\eta = 0.56$) for a homogeneous WDM PDM-QPSK system over a Nx50 km SMF NDM link, and we compare it to the one obtained with in-line dispersion management (DM). We use the nonlinear effects separation procedure[7] to see the rate at which the NLT due to individual self and cross nonlinear effects decreases at increasing N in both NDM and DM cases.

Simulated NDM and DM systems

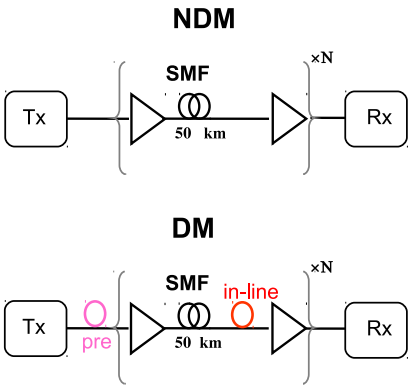

Fig. 1: Block diagrams of NDM and DM simulated systems. TX block represents 19 channels, NRZ-PDM-QPSK modulated at $R = 28$ Gbaud. Propagation uses the SSFM with Manakov nonlinear step.

Fig. 1 shows the block diagram of the simulated NDM and DM links. The transmitter consisted of 19 WDM non-return to zero (NRZ) 28 Gbaud PDM-QPSK channels, with Δf =50 GHz. All channels were modulated with 2^{10} and 2^{14} independent random symbols in the DM and NDM cases, respectively. Each channel was filtered by a supergaussian filter of order 2 with bandwidth $0.9R$. The state of polarization (SOP) of each carrier was randomized on the Poincaré sphere. The transmission line consisted of N spans of 50km of SMF (D =17 ps/nm/km, α =0.2 dB/km, γ =1.3 $W^{-1}km^{-1}$). Propagation used the vector split-step Fourier method (SSFM) with zero polarization mode dispersion and Manakov nonlinear step[7]. In the DM case, an in-line residual dispersion per span (RDPS) of 30 ps/nm and a straight-line rule precompensation[12]

$$D_{pre} = -\frac{D}{\alpha} - \frac{N-1}{2} RDPS \qquad (2)$$

were used. In the coherent receiver we neglected laser phase noise and frequency offset. The standard digital signal processor consisted of a chromatic dispersion compensation block, of a data-aided polarization demultiplexer, and a 27 taps Viterbi and Viterbi phase estimator.

The objective of the simulations was to estimate the NLT $\hat{P}_1$ versus distance when nonlinearities (NL) are selectively activated[7]. The 1dB NLT is obtained from a series of BER Monte Carlo estimations (averaged over input polarization states) at increasing amplifiers noise figure until the target BER_0 is obtained, as detailed in[12]. In the NDM case, noise was all loaded at the receiver since it is known that signal-noise nonlinear interactions are negligible at 28 Gbaud[12]. In the DM case we calculated the NLT both with distributed noise and with noise loading. Using nonlinearity decoupling, we studied the following four cases: 1) single channel (label "SPM" in the following figures); 2) WDM with only scalar XPM active (label "XPM"); 3) WDM with only cross-polarization modulation (label "XPolM") active; 4) WDM with all nonlinearities active (label "WDM").

Simulations were run using the open-source software Optilux[13]. Obtaining the curves presented in each of the following Fig. 2 and Fig. 3 took approximately 3 weeks by running full time on an 8-core Dell processor.

Results

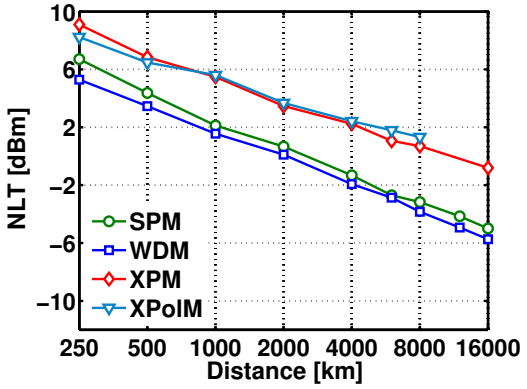

Fig. 2: 1 dB NLT $\hat{P}_1$ vs distance for 19-channel homogeneous 28 Gbaud NRZ PDM-QPSK system with $\Delta f = 50$ GHz over a NDM Nx50km SMF link. No PMD.

NDM system. Fig. 2 shows the corresponding NLT $\hat{P}_1$ versus distance, with span number N ranging from 5 to 320. We first remark that at all distances single-channel effects (SPM) dominate at this $\eta = 0.56$ bandwidth efficiency[9]. The effect of the comparable-size cross-nonlinearities XPM and XPolM on the overall NLT (WDM) is felt only at distances below 2000 km. The reason is that single-channel nonlinearity accumulates at a faster rate than cross-channel nonlinearity. Equation (1) predicts on this log-log plot a NLT decrease with a slope $-x/2$ dB/dB. From Fig. 2 on

the short range up to 2000 km (40 spans) by least mean-square fitting data with straight lines we find $x_{SPM} \cong 1.32$, $x_{XPM} \cong 1.22$, $x_{XPolM} \cong 0.92$ and $x_{WDM} \cong 1.16$, while fitting on the long range (up to 320 spans) we measure $x_{SPM} \cong 1.28$, $x_{XPM} \cong 1.08$, $x_{XPolM} \cong 0.92$ and $x_{WDM} \cong 1.22$. We first note that the long-range x_{WDM} value is consistent with measurements in[8] at the same η, while the short-range x_{SPM} is in agreement with[10]. However, the most novel piece of information we learn from Fig. 2 is that the smaller slope of cross-nonlinearity observed in[10] is an average of the XPolM and XPM slopes, where scalar XPM accumulates at a faster rate. The intuitive reason is easily understood in a completely resonant DM map with RDPS=0. In such a case the walkoff completely realignes the interfering pattern intensities, hence XPM is identical at each span, i.e., it is truly resonant. Instead, the rotations induced by XPolM never bring back to the same starting SOP at each span, hence XPolM is never truly resonant.

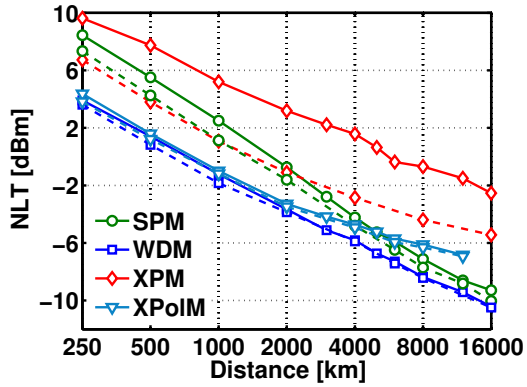

Fig. 3: 1dB NLT vs distance for 19-channel homogeneous 28 Gbaud NRZ PDM-QPSK system with $\Delta f = 50$ GHz over a DM Nx50km SMF link with 30 ps/nm RDPS and distance-optimized SLR precompensation (2). No PMD. Solid lines: ASE noise loading at RX. Dashed lines: distributed ASE.

DM system. It is instructive to also take a look at the same NLT curves in a legacy DM map, as shown in Fig. 3. In the figure we report both the unrealistic case of noise loading (solid lines) and the realistic case of ASE distributed at each amplifier, where nonlinear signal-ASE interactions are fully accounted for (dashed lines). We remark that pre-compensation is here changed at each value of N according to (2), hence the measured NLTs do not truly portray the noise accumulation with N in the *same* line. The figure confirms that[9]:

i) scalar XPM plays a minor role in the PDM-QPSK constant intensity format, and is quite sensitive to signal-noise interactions, here manifested as nonlinear phase noise (NLPN);

ii) single channel (SPM) effects also play a minor role up to about 4000 km, and in that range are also quite sensitive to NLPN;

iiii) the dominant nonlinearity is XPolM up to about 4000 km, but eventually SPM effects become dominant as they accumulate at a faster rate. XPolM is not impacted by signal-ASE interactions.

We note that the slope of SPM in the first 2000 km is about $x_{SPM} \cong 2$, but such a slope decreases at larger distances, since RDPS starts accumulating enough dispersion to make the DM system look more similar to a NDM system. Within the first ∼2000 km we also measure (with NLPN) $x_{XPM} \cong 1.73$ and $x_{WDM} \cong 1.66$. The fact that XPolM is less "resonant" than scalar XPM is seen in the lowering of the local XPolM slope after 2000 km. However note that in order to correctly reproduce the XPolM NLT we had to use random modulating sequences of 2^{10} symbols on each channel, since shorter sequences correctly reproduced XPM but caused the XPolM NLT to level off at too small values of N. For NDM systems even longer sequences are required since the system "memory" is much longer.

Conclusions

We have shown that in NDM systems the nonlinear interference accumulation rate x can also be measured through the nonlinear threshold decrease rate, and we have provided the accumulation rates of the individual self- and cross-channel effects, corroborating and complementing recent simulation and lab results[5,8,10].

References

1 P. Poggiolini et al., Photon. Technol. Lett. **23**, 742 (2011).
2 E. Grellier et al., Opt. Exp. **19**, 12781 (2011).
3 A. Carena et al., J. Lightw. Technol. **30**, 1524 (2012).
4 A. Bononi et al., Opt. Exp. **20**, 7777 (2012).
5 F. Vacondio et al., Opt. Exp. **20**, 1022 (2012).
6 A. Carena et al., Proc. ECOC'10 P4.07 (2010).
7 A. Bononi et al., Proc. ECOC'10 Th.10.E.1 (2010).
8 O. V. Sinkin et al., Proc. OFC'12 OTu1A.2 (2012).
9 A. Bononi et al., Proc. OFC'11 OW07 (2011).
10 O. Rival et al., Proc. OFC'12 JW2A.52 (2012).
11 Y. Ye et al., Proc. OFC'12 JW2A.45 (2012)
12 A. Bononi et al., Opt. Fiber Technol. **16**, 73 (2010).
13 "Optilux Toolbox", www.optilux.sourceforge.net